ACS APPLIED MATERIALS & INTERFACES

Research Article

www.acsami.org

Three-Dimensional Triple Hierarchy Formed by Self-Assembly of Wax Crystals on CuO Nanowires for Nonwettable Surfaces

Jun-Young Lee,[○,†,‡] Sasha Pechook,[○,§,⊥] Deok-Jin Jeon,[†] Boaz Pokroy,[§,⊥] and Jong-Souk Yeo*[,†,‡]

[†]School of Integrated Technology, Yonsei University, 162-1, Veritas Hall C, Songdo-dong, Yeonsu-gu, Incheon 406-840, Rep. of Korea

[‡]Yonsei Institute of Convergence Technology, Yonsei University, Incheon 406-840, Rep. of Korea

[§]Department of Materials Science and Engineering and [⊥]Russell Berrie Nanotechnology Institute, Technion−Israel Institute of Technology, Haifa 32000, Israel

Supporting Information

ABSTRACT: Novel hierarchical surfaces combining paraffin wax crystals and CuO nanowires are presented. We demonstrate a bioinspired hierarchical wax on nanowire (NW) structures having high water and ethylene glycol repellence. In general, vertically grown nanowire arrays can provide a superhydrophobic surface (SHS) due to extremely high surface roughness but cannot repel ethylene glycol. In this paper, $C_{36}H_{74}$ and $C_{50}H_{102}$ waxes are thermally evaporated on the surface of CuO NWs, forming highly ordered, three-dimensional (3D) hierarchical structures via self-assembly of wax crystals. These two and three level hierarchical structures provide perfect self-cleaning characteristics, with water contact angles (CAs) exceeding 170°. Furthermore, $C_{36}H_{74}$ and $C_{50}H_{102}$ wax crystals assembled perpendicularly to the longitudinal NW axis form a re-entrant (that is, a multivalued surface topography) curvature enabling high repellence to ethylene glycol (EG) with CAs exceeding 160°. We analyze the wettability dependence on wax crystal size and structure for the optimization of nonwettable hierarchical structured surfaces.

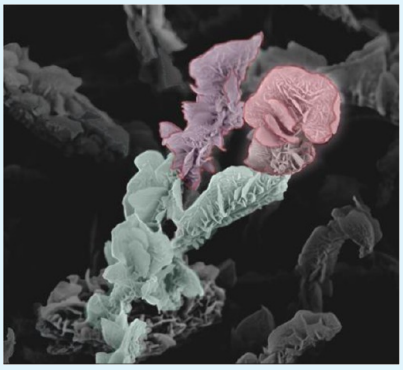

KEYWORDS: *superhydrophobic surfaces, biomimetics, hierarchical structures, nanowires, self-assembly*

INTRODUCTION

Nature is abundant with surfaces possessing unique properties of wettability, such as self-cleaning represented by the lotus leaf,[1] water-repellence of water-strider's legs, water gathering characteristics of a beetle's back, and the superoleophobic[2] nature of a springtail.[3] Since the discovery of the lotus effect, a variety of biological surfaces with unique wetting characteristics have been investigated in order to mimic them.[1] Due to the development of nanotechnology, it became possible to fabricate various nanoscale textured surfaces such as vertically grown nanopillars,[4] nanoparticles,[5] microfibers, and nanoporous structures[6] for outstanding wettability with a variety of width, height, pitch, and number density of the structures. All of the above-mentioned structures possess self-cleaning properties due to the formation of air pockets between the structure and liquid, (Cassie state) which results in high contact angles (>150°) and low contact angle hysteresis.[7−10] On such surfaces, contaminants are automatically eliminated while water droplets roll off the surface keeping the surfaces dry and clean for a long time.[1,10,11]

The self-cleaning characteristic of the lotus leaf stems from its hierarchical structure. The lotus leaf consists of micropapillae which are covered by epicuticular wax crystalline structures.[1,12] Moreover, a previous study has shown that only the areas that consist of hierarchical structures demonstrated superhydrophobic behavior.[1] As to mimic these surfaces, various methods and materials were used to fabricate artificial hierarchically structured surfaces, such as a surface consisting of a Si micropillar array covered by the epicuticular wax extracted from wheat plants.[12,13] On the hierarchical surface, the fraction of local areas at the solid−liquid interface decreases dramatically when air is trapped between the structures,[11−17] thus increasing the water contact angle (CA) and decreasing the CA hysteresis.[18,19] The pressure distributed upon multiscale textures allows the microtexture to repel relatively large droplets without damaging the structure while simultaneously allowing nanostructures to easily repel relatively small droplets.[20] Using these advantages, the hierarchical structure can improve the durability of the surface and prolong the life expectancy with respect to the functionality of the surface.

In addition, there is an increasing scientific and industrial interest in multifunctional characteristics, not only with regard to the hydrophilic and hydrophobic properties but also amphiphobic and omniphobic properties. Omniphobic/oleophobic surfaces can repel, in addition to water, liquids with low surface tension, such as oils and alcohols. In order to achieve

Received: December 25, 2013
Accepted: March 6, 2014
Published: March 6, 2014

   dx.doi.org/10.1021/am4059759 | ACS Appl. Mater. Interfaces 2014, 6, 4927−4934

oleophobic properties, the formation of pillar or papillae-like structures having hydrophobic properties with large surface roughness is not sufficient. The structure should provide convex or re-entrant curvature in order to form an oleophobic surface.[2,21−27] At the edge of the re-entrant structure, the angle between oil−solid interface and oil−air interface is usually lower than 90°, but due to the re-entrant shape, the contact angle of the entire oil droplet becomes larger than 90° as a metastable state. Especially, when the oil contact angle becomes larger than 150°, the surface is called superoleophobic. Fabrication of amphiphobic or omniphobic surfaces that have superhydrophobic and superoleophobic properties is a key to making perfect self-cleaning surfaces.

Recently, many research groups demonstrated various superoleophobic surfaces. In addition, various functional surfaces with unique wettability have been used for many applications such as superhydrophobic surfaces for heat transferring,[28−32] the prevention of ice formation,[33−38] non-adhesiveness and antifouling,[39] superhydrophilic−superoleophobic surfaces for oil−water separations,[40,41] and super-omniphobic surfaces for chemical shielding.

Various waxes were used for the fabrication of superhydrophobic surfaces. One of the frontier researches of wax crystal was conducted by Koch et al. They extracted wax from plants and deposited it on various substrates using thermal evaporation.[42,43] Bhushan et al. fabricated hierarchical surfaces using thermal evaporation of synthetic paraffin wax (hexatriacontane) on epoxy resin pillars.[44] Wax covered surfaces naturally have sufficiently high roughness which can provide hydrophobic characteristics. Pechook et al. studied the time-dependent change of roughness and crystallinity of thermally evaporated *n*-hexatriacontane wax ($C_{36}H_{74}$).[45] They showed that the initial thermally evaporated $C_{36}H_{74}$ layer undergoes significant roughening by crystal growth at room temperature within a few days and fast roughening at elevated temperatures (40 °C). The deposited layers were highly crystalline with extremely strong preferred orientation in the (1 1 0) direction.[44−46] Stable crystalline wax layers with tunable roughness can be deposited on various substrates. Hierarchical wax structures can be fabricated using waxes with various chain lengths in sequential deposition process (small wax crystals with large molecular weight were deposited on large wax crystals with small molecular weight). Such structures have improved repellence of water and low surface tension liquids.[46]

Several studies suggested vertically grown CuO nanowire or nanopillar arrays modified with low surface energy materials as water repellent surfaces.[47−50] A study by Guo at al. demonstrated the fabrication of ZnO/CuO heterohierarchical nanotrees on Cu substrates for the formation of self-cleaning hydrophobic surfaces.[50] Advancing these hierarchical structures further, we fabricated wax on nanowire hierarchical structures (Scheme 1) for the improvement of lower surface tension liquids repellence (The liquid of choice was ethylene glycol due to its intermediate surface tension characteristics) and determination for an optimal combination of oxide nanowire and nanoscale paraffin wax crystal for this purpose.

EXPERIMENTAL SECTION

CuO Nanowire Growth. Copper foils were ultrasonically cleaned in ethanol, acetone, and deionized water (DI) for 15 min. CuO nanowires were fabricated on precleaned Cu foils. Cut copper foils (4 cm × 4 cm) were cleaned in 4 M HCl for 5 s, rinsed in DI water for 5 min, and then, oxidized in an ammonium ambient solution of 2.5 M NaOH and 0.1 M $(NH_4)_2S_2O_8$ at 4 °C for 10 and 60 min.[51,52] Then samples were rinsed using DI water 5 times and dried at 180 °C for 2 h on a hot plate. While it was dried, the $Cu(OH)_2$ nanostructure was transformed to CuO nanowire by dehydration reaction.

Scheme 1. (a) Unary CuO Nanowire Surface, (b) Hierarchical Wax on a Nanowire Surface, and (c) a Three Level Hierarchical Structure Formed by $C_{50}H_{102}$ Wax Crystals

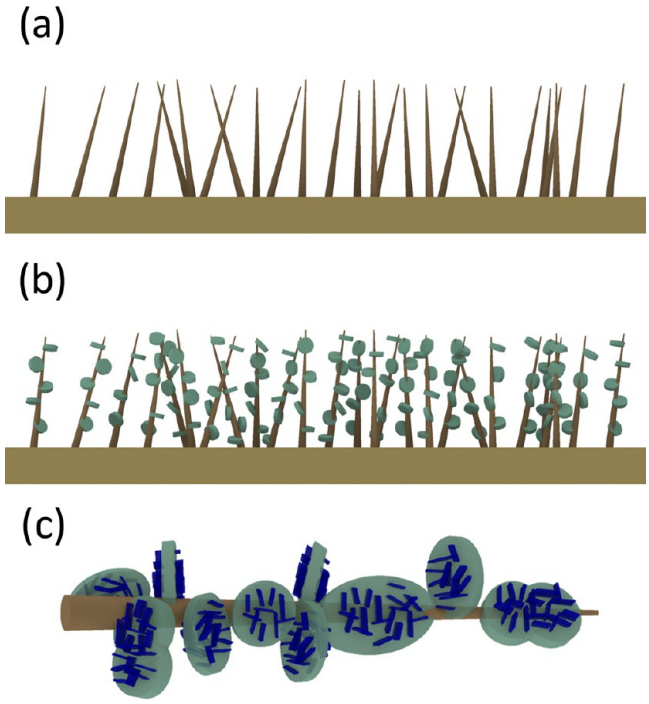

As-prepared nanowire surface can be used as a reference unary structure to compare with the hierarchical structure after SAMs surface modification. In order to provide hydrophobic properties to the NWs, the surface was chemically modified by a self-assembled monolayer (SAM) of *n*-octadecylphosphonic acid ($C_{17}H_{38}O_3P$, Alfa Aesar). Samples were immersed in 3 mM SAM solution (ethanol 200 proof) for 36 h. Samples were rinsed in ethanol and DI water followed by drying in air prior to CA measurements.

Wax Deposition on CuO Nanowires. For the formation of wax on CuO nanowire textured surfaces, pentacontane wax ($C_{50}H_{102}$) (Sigma-Aldrich) and hexatriacontane wax ($C_{36}H_{74}$) (Sigma-Aldrich) were thermally evaporated via Moorfield MiniLab evaporator. The deposition procedure was conducted in a vacuum chamber at 6×10^{-6} mbar. Samples were positioned on a holder 10−12 cm above a crucible loaded with 40−50 mg of wax (40 mg of $C_{36}H_{74}$ and 50 mg of $C_{50}H_{102}$). The system was slowly heated from 70 to 100 °C, and evaporation occurred at ∼100 °C during a 15 min time period. Evaporated specimens were transferred and cooled down to a room temperature (25 °C).

Characterization. Surface morphology was characterized via field emission scanning electron microscopy (FE-SEM, JSM-7100F, JEOL, Japan) and high-resolution scanning electron microscopy (Zeiss Ultra Plus HR-SEM). X-ray diffraction analysis (XRD, Smartlab X-ray Diffractometer, Rigaku, Japan) was conducted on CuO nanowire grown surfaces, wax deposited surfaces, and hierarchical surfaces to confirm the crystallization of polycrystalline CuO and single crystalline waxes. Wettability of the surfaces was measured using contact angle measurement systems (Dataphysics, OCA15EC, Germany and Attension theta tensiometer) with DI water and ethylene glycol with 7 μL DI water/ethylene glycol droplets at room temperature (RT).

The contact angle (CA) and CA hysteresis of each liquid were measured for each combination of hierarchical structures with CuO nanostructures and two different kinds of waxes. The static CAs and

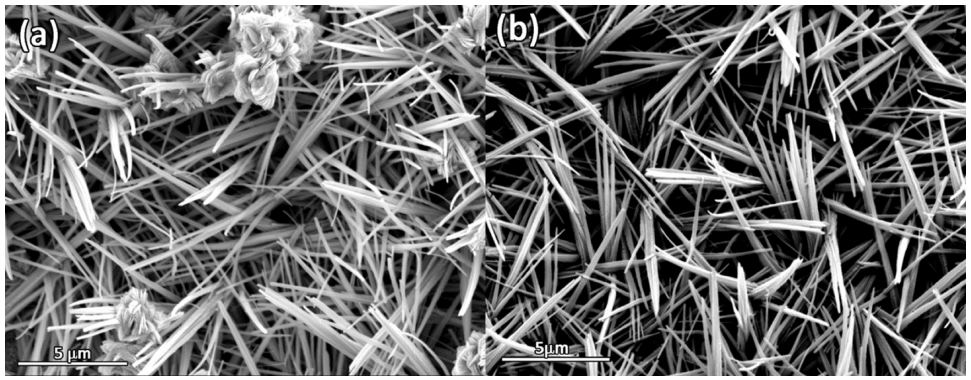

Figure 1. SEM images of CuO nanowires grown by solution method oxidized for (a) 10 and (b) 60 min.

CA hysteresis (CAH) were measured and averaged over ten times. CAH on various surfaces was measured by continuous liquid injection and retraction for the assessment of advancing and receding contact angles. Evaporation experiments were performed with 7 μL DI water droplets at RT.

RESULTS AND DISCUSSION

In this research, a re-entrant structure was fabricated on CuO nanowires using hexatriacontane ($C_{36}H_{74}$) and pentacontane ($C_{50}H_{102}$) paraffin waxes in order to achieve high repellence with ethylene glycol and to analyze the dependence of wax crystal size on wettability. As schematically presented in Scheme 1, we grew CuO nanowires on Cu foil and deposited *n*-paraffin waxes on the NW structure. CuO nanowires are of high aspect ratio combined with tight packing leading to high surface roughness. In addition, the NWs are chemically stable and thus are applicable as a stable base of multilevel hierarchical structures.

Hierarchical Wax on CuO Nanowire Structure. In order to enhance surface wettability and achieve liquid repulsion with low surface tension liquids (<72.2 mN/m), we investigated a hierarchical structure composed of CuO nanowires and wax crystals. As shown in Figure 1, CuO nanowires were grown randomly on Cu foil by the ammonium ambient solution method. The ammonium ambient solution method involves immersion of precleaned Cu foils in sodium hydroxide and ammonium persulfate solution. First, Cu was converted to copper hydroxide in the solution. Then, copper hydroxide was transformed to copper oxide while drying at 180 °C. CuO nanowires were characterized using a field emission scanning electron microscope (FE-SEM).

Copper oxide nanowires had an average length of 8 and 10 μm and an average diameter of 150 and 100 nm at different immersion times of 10 and 60 min, respectively, as shown in Table 1. Increasing immersion time had two main effects: (1) The length was increased while the diameter was reduced, thus increasing the aspect ratio of the NWs. (2) The amount of nanowires was increased as observed in XRD spectra (Figure 2a). This increase was indicated by the increase of the CuO peaks (integrated area) as compared to the Cu substrate peak. Both density and aspect ratio of surface features have an effect on wetting properties.[53] These properties would be further examined for the unary CuO NW and the NW−wax hierarchical structures. As seen in Figure 2a, the CuO nanowires are of monoclinic structure. The main diffraction peaks observed are of the (002) and (111) planes indicating rather ordered formation of the CuO NW. To measure the wettability of unary CuO nanostructure, we modified the surface properties using self-assembled monolayer (SAM) forming a surface layer of CH_3 which energetically resembles the paraffin wax (intrinsic wettability). Contact angle measurement with DI water and ethylene glycol were performed on the modified surfaces. The high aspect ratio (over 60) combined with the low surface-energy modification resulted in extremely high water contact angles and very low CAH indicating self-cleaning characteristics. The higher aspect ratio NW (60 min immersion) was slightly beneficial for water repellence where the main advantage of the higher aspect ratio was observed for EG contact angle (154° for $CuO_{60\ min}$ and 125° for $CuO_{10\ min}$).

Table 1. Average Length and Diameter of CuO Nanowires and Wax Crystalline Structures on CuO NW

structure	length (μm)	length (μm) (secondary structure)	diameter/ thickness(nm)
CuO NWs (10 min)	6−10		100−200
CuO NWs (60 min)	8−10		50−100
$C_{36}H_{74}$ wax on NW	1	0.5	100
$C_{50}H_{102}$ wax on NW	0.9−1	0.1	20

Hierarchical CuO−wax samples were prepared as follows: $C_{36}H_{74}$ and $C_{50}H_{102}$ waxes were thermally evaporated on the surfaces of CuO nanowires prepared at two different immersion times (10 and 60 min). After deposition, the samples were kept at room temperature (RT). Wax crystals were formed via self-assembly without inducing any damage to the CuO nanowires. The hierarchical structures of $C_{36}H_{74}$ and $C_{50}H_{102}$ wax crystals on CuO nanowires are presented in Figure 3. $C_{36}H_{74}$ wax crystals are tightly arranged on the nanowires aligned parallel and perpendicular to the nanowire backbone, with similar crystal size (Figure 3a and b). Similar tight crystal alignment was observed for the $C_{50}H_{102}$ wax, where the main difference was the crystal size; $C_{50}H_{102}$ formed a hierarchical structure composed of large and small crystals (1 μm and 100 nm, respectively), producing an additional third hierarchy level (Figure 3c and d). For both cases, $C_{36}H_{74}$ and $C_{50}H_{102}$, liquid placed on the surface will contact only wax crystals without any contact with the CuO NWs resulting in low surface energy, necessary for high contact angles. Thermally evaporated paraffin wax crystalline layers present strong preferred orientation of the (110) and (200) planes,[45,46] and the same preferred orientation (2-theta peaks of the waxes are observed at 21.6° and 23.9°) was observed for the wax crystals deposited

dx.doi.org/10.1021/am4059759 | ACS Appl. Mater. Interfaces 2014, 6, 4927−4934

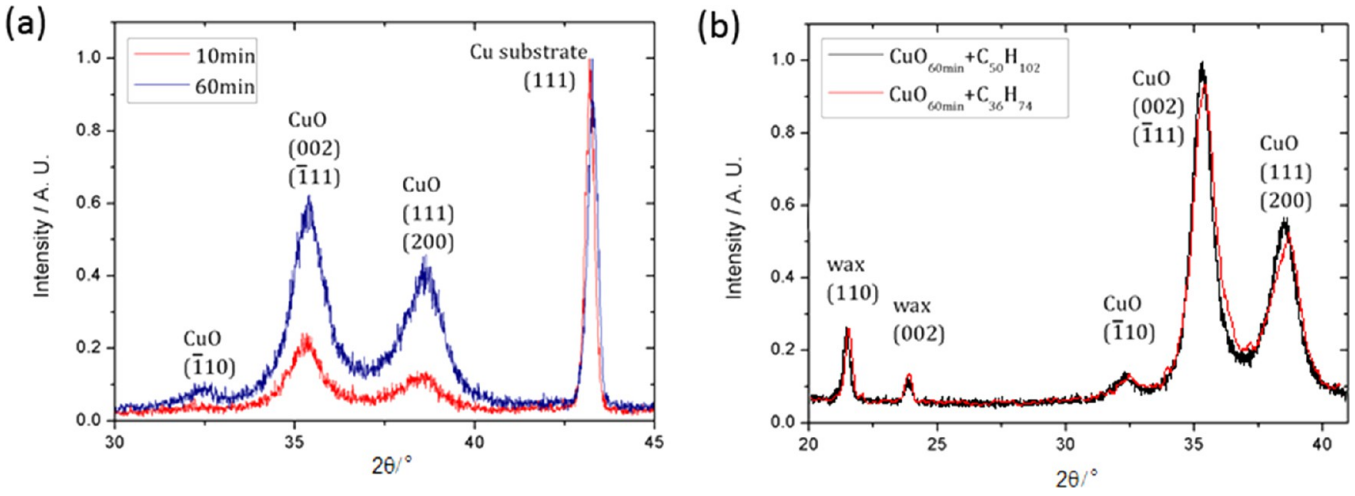

Figure 2. XRD spectrum of (a) CuO nanowires with two different oxidation times of 10 and 60 min and (b) $C_{36}H_{74}$ and $C_{50}H_{102}$ wax on CuO NW oxidized for 60 min.

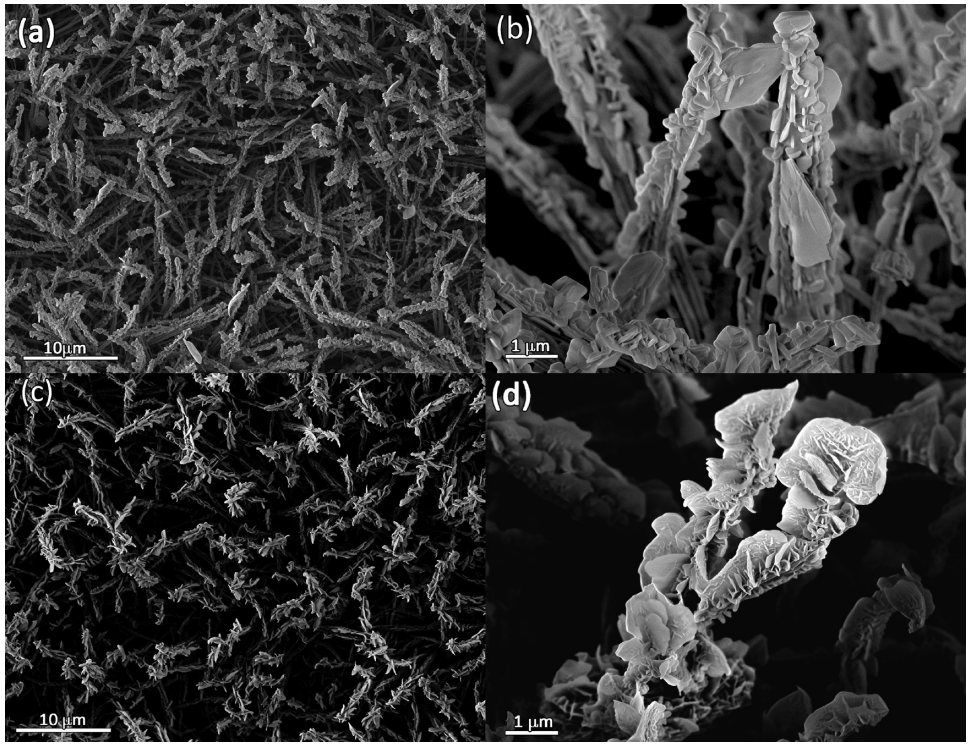

Figure 3. SEM images of (a and b) $C_{36}H_{74}$ wax on CuO NWs (oxidized for 60 min) and (c and d) $C_{50}H_{102}$ wax on CuO NWs (oxidized for 60 min). (b and d) Taken at a tilt angle of 40°.

on CuO nanowires (Figure 3b). When deposited on a flat surface, $C_{36}H_{74}$ wax crystals had an average length of 1.3 μm and an average width of 100 nm and $C_{50}H_{102}$ crystals had an average length of 1 μm and an average width of 20 nm. When deposited on CuO NW, $C_{36}H_{74}$ wax crystals still maintained similar dimensions whereas $C_{50}H_{102}$ crystals demonstrated two different size scales: the first size similar to that deposited on a flat surface but the second one an order of magnitude smaller in size, as summarized in Table 1. The multilevel hierarchical structure of combined CuO nanowires and wax crystals results in a re-entrant curvature, which in turn reduces the wettability of the surface for low surface tension liquids.[2,21−27]

Water CA. Static water contact angle analysis revealed that both wax and SAMs modified CuO unary surfaces were superhydrophobic due to the combination of surface roughness (wax crystals/CuO NW) and low surface energy originated from the surface modification with SAMs or the intrinsic hydrophobicity of paraffin wax. For unary structures, aspect ratio of roughness features had an effect on surface wettability; the lower aspect ratio features from $C_{50}H_{102}$ crystals or $CuO_{10\ min}$ NW have shown lower static contact angles compared to high aspect ratio features from $C_{36}H_{74}$ or $CuO_{60\ min}$ NW, respectively. All hierarchical structures had similar results for static and dynamic CA measurements (Table 2) indicating the elimination of aspect ratio effect from the first hierarchy level in the unary structure. As a result, the differences observed in height/radius values for different nanowires ($CuO_{10\ min}$ and $CuO_{60\ min}$) have shown little influence on CA

dx.doi.org/10.1021/am4059759 | ACS Appl. Mater. Interfaces 2014, 6, 4927−4934

Table 2. CA and CAH Measurements for Various Substrates[a]

structure	water CA (deg)	CAH (deg)	ethylene glycol CA (deg)	CAH (deg)
unary $C_{36}H_{74}$ wax	170	3	128	25
unary $C_{50}H_{102}$ wax	164	9	103	30
CuO_{10min} + SAMs	167	2	125	22
CuO_{60min} + SAMs	>170	2	154	20
CuO_{10min} + $C_{50}H_{102}$	>170	2	165	9
CuO_{60min} + $C_{50}H_{102}$	>170	2	165	6
CuO_{10min} + $C_{36}H_{74}$	>170	2	154	6
CuO_{60min} + $C_{36}H_{74}$	165	3	160	9

[a]Static CA measurements were performed with a 7 μL droplet, and dynamic measurements were performed by varying drop volume from 7 to 15 μL and to 7 μL. All experiments were performed at room temperature.

and CAH values when a second hierarchy level was added. The hierarchical surfaces have shown extremely high contact angles (>170°) and extremely low CAH (<3°) which are beneficial for self-cleaning applications. The contact angles on the textured surface with hierarchical structure can be calculated by the Cassie–Baxter model[9,18,54,55] as follows:

$$\cos\theta_n^* = (1 - f_{LV,n})\cos\theta_{n-1}^* - f_{LV,n^*}$$

Here, f_{LV} is the area fraction of the liquid–vapor interface, n is the number of levels in hierarchical structures, and $f_{LV,n}$ is the f_{LV} of the nth level of structures.[51] Due to the large area fraction of the liquid–vapor interface and small area fraction of the liquid–solid interface, contact angle of the hierarchical surface increases in accordance with the increasing n. Wax on nanowire hierarchical structures provide higher contact angle than unary NW structures and, thus, are beneficial for superhydrophobic applications.

Additional CA measurements during an evaporation process were performed in order to assess the stability of the surface, i.e., the stability of Cassie state with decreasing droplet volume. The droplet curvature might be responsible for the transition to the homogeneous wetting state (Wenzel). The Laplace pressure (decreasing droplet volume results in increased pressure) determines this curvature. The measurements were performed with decreasing droplet volume (7–0.1 μL) of DI water, as presented in Figure 4. It is clearly seen that the hierarchical surface remained in the Cassie wetting state for significantly smaller droplets compared to unary surfaces (~5.5 and 3.5 μL for $C_{36}H_{74}$ and $CuO_{60\ min}$ + SAMs and <0.5 μL for $CuO_{60\ min}$ + wax structures). This effect can be attributed to the second hierarchy level crystals hindering the transition via two possible mechanisms: (1) the crystals are pinning the contact line preventing the liquid from filling the air pockets and (2) the effect of size dependent wettability is reduced by the nanoscale crystals supporting smaller droplets.

Wettability of Hierarchical Surfaces with Ethylene Glycol. In order to examine wetting properties of ethylene glycol on our surfaces, CA and CAH measurements were performed with 7 μL droplets of ethylene glycol (EG, γ_{LV} = 47.3 mN/m). The measured surfaces were $C_{17}H_{38}O_3P$ coated CuO nanowires, wax on flat Cu foils, and wax on CuO NW hierarchical structures. The results are presented in Table 2. All unary surfaces had high CAH with EG due to pinning effect. CAs had a general trend of increasing values with increasing aspect ratio; EG CA on $C_{50}H_{102}$ wax crystals (lowest aspect ratio) was as low as 108°, on CuO_{10min} NW was 125° and on CuO_{60min} NW (highest aspect ratio) was as high as 154°. The observed trend indicates the importance of high aspect ratio features for keeping air trapped between roughness features. The large height of (~9 μm) roughness features prevents droplet droop from exceeding the asperities height (once it occurs, a transition to a Wenzel state will occur), maintaining the droplet in a Cassie wetting state.[56] Low CAs and high CAH are a result of EG penetration to surface grooves by hemiwicking force. For the hierarchical structures combining CuO NW with wax crystals, EG contact angles exceeded 150°. Additionally CAH was lower than 10°, enabling self-cleaning (Figure S1 Supporting Information) with EG on all examined hierarchical surfaces. Exceptional results were observed for $C_{50}H_{102}$ crystals on CuO_{10min}/CuO_{60min} NW with EG CA as high as 165°. The low values of CAH and high CAs were achieved for the hierarchical structures, which indicate a Cassie wetting state enabled by the re-entrant structure of the perpendicularly aligned wax crystals on NW longitudinal axis. This is shown in a cross-sectional SEM image and a schematic figure (Figure 5). Higher CAs achieved for $C_{50}H_{102}$ hierarchical structure as compared to $C_{36}H_{74}$ structure can be explained by the difference in wax structures; $C_{36}H_{74}$ crystals form a 3D structure on the NWs composed of parallel and perpendicularly aligned crystals where both parallel and perpendicular crystal are of similar dimensions resulting in a two scale hierarchical structure.

Close examination of $C_{50}H_{102}$ crystals on CuO NW (Figure 3d) reveals a third hierarchy level; small crystals (1 order of magnitude smaller than the large crystals) randomly aligned on the large crystals. It has been previously shown that the presence of nanoscale roughness features contribute to the stabilization of hydrophobic state and improve the ability to support low surface tension liquids.[46,57,58] Indeed the combination of reduced crystal thickness (20 nm for $C_{50}H_{102}$ crystals compared to 100 nm for $C_{36}H_{74}$ crystals) and the

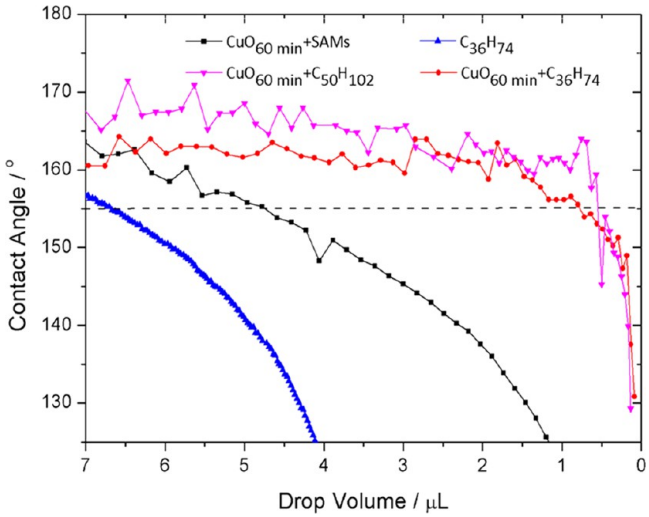

Figure 4. Static contact angle values as a function of droplet volume (data presented for water).

dx.doi.org/10.1021/am4059759 | ACS Appl. Mater. Interfaces 2014, 6, 4927–4934

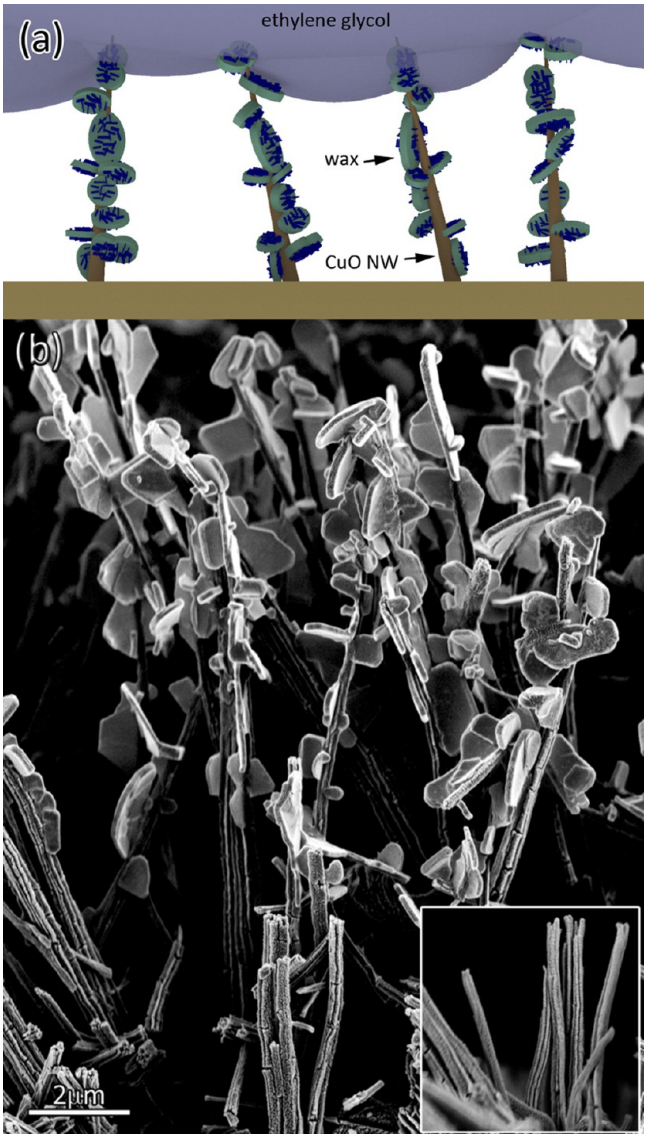

Figure 5. (a) Schematic representation of ethylene glycol droplet on 3D hierarchical structure and (b) cross-sectional HRSEM image of $CuO_{60min}/C_{36}H_{74}$. (inset) $CuO_{60\ min}$ NW at the same magnification.

presence of additional nanoscale, hierarchy level results in reduction of the contact area between the applied liquid and the substrate (f_{SL}), thus leading to elevated contact angles. According to wetting measurements, the presence of a third hierarchy level eliminates the effect of aspect ratio in the first hierarchy level, which can still be observed for a two level hierarchical structure (CA of 154° for $CuO_{10\ min}/C_{36}H_{74}$ and CA of 160° for $CuO_{60\ min}/C_{36}H_{74}$). Wetting experiments with EG droplet volume diminishing from 7 to 1 μL revealed no effect of droplet volume on CA values (Supporting Information Figure S2) measured on the hierarchical structures, indicating the surface stability for a range of droplet volumes.

CONCLUSIONS

We investigated a nanoscale hierarchical structure composed of CuO nanowire and *n*-paraffin wax crystals. This nanoscale wax on nanowire hierarchical structure demonstrates extremely high water contact angles, exceeding 170°, and extremely low contact angle hysteresis. Furthermore, due to the re-entrant curvature achieved with the formation of wax crystals on oxide nanowire, the hierarchical structure provides contact angles of 165° and low CAH (of <6°) with ethylene glycol, thus resulting in Cassie state. This result can potentially provide an oleophobic surface. Ethylene glycol repellence depends on wax crystal size and the number of size scales achieved. Since paraffin wax can be easily coated on any substrate, these findings can be extended to other nanostructures such as hydrothermally grown nanorods, plasma treated polymer nanostructures, and electro-spun nanofibers. The pitch and density of nanowires can be controlled using a variety of conventional top-down and bottom-up approaches to optimize the results further based on hierarchical structures.

ASSOCIATED CONTENT

Supporting Information

Cross-sectional analysis and self-cleaning effect of hierarchical structure as noted in text. This material is available free of charge via the Internet at http://pubs.acs.org.

AUTHOR INFORMATION

Corresponding Author

*E-mail: jongsoukyeo@yonsei.ac.kr.

Author Contributions

○J.-Y.L. and S.P. contributed equally to this work.

Notes

The authors declare no competing financial interest.

ACKNOWLEDGMENTS

This research was supported by the MSIP (Ministry of Science, ICT and Future Planning), Korea, under the "IT Consilience Creative Program" (NIPA-2014-H0201-14-1001) supervised by the NIPA (National IT Industry Promotion Agency). We thank Dr. Iryna Polishchuk from the Department of Materials Engineering at the Haifa Technion helping with the thermal deposition.

REFERENCES

(1) Neinhuis, C.; Barthlott, W. Characterization and Distribution of Water-repellent, Self-cleaning Plant Surfaces. *Ann. Bot.* **1997**, *79* (6), 667−677.

(2) Tsujii, K.; Yamamoto, T.; Onda, T.; Shibuichi, S. Super Oil-repellent Surfaces. *Angew. Chem., Int. Ed. Engl.* **1997**, *36* (9), 1011−1012.

(3) Helbig, R.; Nickerl, J.; Neinhuis, C.; Werner, C. Smart Skin Patterns Protect Springtails. *PloS One* **2011**, *6* (9), e25105.

(4) Dorrer, C.; Rühe, J. Some thoughts on superhydrophobic wetting. *Soft Matter* **2009**, *5* (1), 51−61.

(5) Bravo, J.; Zhai, L.; Wu, Z.; Cohen, R. E.; Rubner, M. F. Transparent superhydrophobic films based on silica nanoparticles. *Langmuir* **2007**, *23* (13), 7293−7298.

(6) Yao, X.; Hu, Y.; Grinthal, A.; Wong, T.-S.; Mahadevan, L.; Aizenberg, J. Adaptive Fluid-infused Porous Films with Tunable Transparency and Wettability. *Nat. Mater.* **2013**, *12* (6), 529−34.

(7) Quéré, D. Wetting and Roughness. *Annu. Rev. Mater. Res.* **2008**, *38* (1), 71−99.

(8) Cassie, A. B. D.; Baxter, S. Wettability of Porous Surfaces. *Trans. Faraday Soc.* **1944**, *40*, 546−551.

(9) Cassie, A. B. D. Contact Angles. *Discuss. Faraday Soc.* **1948**, *3*, 11−16.

(10) Quéré, D. Non-sticking Drops. *Rep. Prog. Phys.* **2005**, *68* (11), 2495−2532.

(11) Li, X.-M.; Reinhoudt, D.; Crego-Calama, M. What Do We Need for a Superhydrophobic Surface? A Review on the Recent Progress in the Preparation of Superhydrophobic Surfaces. *Chem. Soc. Rev.* **2007**, *36* (8), 1350−68.

(12) Koch, K.; Bohn, H. F.; Barthlott, W. Hierarchically Sculptured Plant Surfaces and Superhydrophobicity. *Langmuir* **2009**, *25* (24), 14116−20.
(13) Jung, Y. C.; Bhushan, B. Mechanically Durable Carbon Nanotube-Composite Hierarchical Structures with Superhydrophobicity, Self-Cleaning, and Low-Drag. *ACS Nano* **2009**, *3* (12), 4155−4163.
(14) Nosonovsky, M. Multiscale Roughness and Stability of Superhydrophobic Biomimetic Interfaces. *Langmuir* **2007**, *23* (6), 3157−3161.
(15) Marmur, A. From Hygrophilic to Superhygrophobic: Theoretical Conditions for Making High-contact-angle Surfaces from Low-contact-angle Materials. *Langmuir* **2008**, *24* (14), 7573−7579.
(16) Roach, P.; Shirtcliffe, N. J.; Newton, M. I. Progess in Superhydrophobic Surface Development. *Soft Matter* **2008**, *4* (2), 224.
(17) Gao, L.; McCarthy, T. J. The "Lotus Effect" Explained: Two Reasons Why Two Length Scales of Topography Are Important. *Langmuir* **2006**, *22* (7), 2966−2967.
(18) Herminghaus, S. Roughness-induced Non-wetting. *Europhys. Lett.* **2007**, *79* (5), 165.
(19) Johnson, R. E. J.; Dettre, R. H. Contact Angle Hysteresis. III. Study of an Idealized Heterogeneous Surface. *J. Phys. Chem.* **1964**, *68* (7), 1744−50.
(20) Watson, G. S.; Cribb, B. W.; Watson, J. A. How Micro/Nanoarchitecture Facilitates Anti-Wetting: An Elegant Hierarchical Design on the Termite Wing. *ACS Nano* **2010**, *4* (1), 129−136.
(21) Tuteja, A.; Choi, W.; Ma, M.; Mabry, J. M.; Mazzella, S. A.; Rutledge, G. C.; McKinley, G. H.; Cohen, R. E. Designing Superoleophobic Surfaces. *Science* **2007**, *318* (5856), 1618−22.
(22) Tuteja, A.; Choi, W.; Mabry, J. M.; McKinley, G. H.; Cohen, R. E. Robust Omniphobic Surfaces. *Proc. Natl. Acad. Sci. U.S.A.* **2008**, *105* (47), 18200−5.
(23) Ahuja, A.; Taylor, J. A.; Lifton, V.; Sidorenko, A. A.; Salamon, T. R.; Lobaton, E. J.; Kolodner, P.; Krupenkin, T. N. Nanonails: A Simple Geometrical Approach to Electrically Tunable Superlyophobic Surfaces. *Langmuir* **2008**, *24* (1), 9−14.
(24) Deng, X.; Mammen, L.; Butt, H.-J.; Vollmer, D. Candle Soot as a Template for a Transparent Robust Superamphiphobic Coating. *Science* **2012**, *335* (6064), 67−70.
(25) Tuteja, A.; Choi, W.; McKinley, G. H.; Cohen, R. E.; Rubner, M. F. Design Parameters for Superhydrophobicity and Superoleophobicity. *MRS Bull.* **2008**, *33* (8), 752−758.
(26) Chhatre, S. S.; Choi, W.; Tuteja, A.; Park, K.-C.; Mabry, J. M.; McKinley, G. H.; Cohen, R. E. Scale Dependence of Omniphobic Mesh Surfaces. *Langmuir* **2010**, *26* (6), 4027−35.
(27) Kota, A. K.; Li, Y.; Mabry, J. M.; Tuteja, A. Hierarchically Structured Superoleophobic Surfaces with Ultralow Contact Angle Hysteresis. *Adv. Mater.* **2012**, *24* (43), 5838−43.
(28) Chen, C.-H.; Cai, Q.; Tsai, C.; Chen, C.-L.; Xiong, G.; Yu, Y.; Ren, Z. Dropwise Condensation on Superhydrophobic Surfaces with Two-tier Roughness. *Appl. Phys. Lett.* **2007**, *90* (17), 173108.
(29) Boreyko, J.; Chen, C.-H. Self-Propelled Dropwise Condensate on Superhydrophobic Surfaces. *Phys. Rev. Lett.* **2009**, *103*, 184501.
(30) Enright, R.; Miljkovic, N.; Al-Obeidi, A.; Thompson, C. V.; Wang, E. N. Condensation on Superhydrophobic Surfaces: the Role of Local Energy Barriers and Structure Length Scale. *Langmuir* **2012**, *28* (40), 14424−32.
(31) Miljkovic, N.; Enright, R.; Wang, E. N. Effect of Droplet Morphology on Growth Dynamics and Heat Transfer during Condensation on Superhydrophobic Nanostructured Surfaces. *ACS Nano* **2012**, *6* (2), 1776−1785.
(32) Miljkovic, N.; Enright, R.; Nam, Y.; Lopez, K.; Dou, N.; Sack, J.; Wang, E. N. Jumping-droplet-enhanced Condensation on Scalable Superhydrophobic Nanostructured Surfaces. *Nano Lett.* **2012**, *13* (1), 179−87.
(33) Cao, L.; Jones, A. K.; Sikka, V. K.; Wu, J.; Gao, D. Anti-icing Superhydrophobic Coatings. *Langmuir* **2009**, *25* (21), 12444−8.
(34) Kulinich, S. A.; Farzaneh, M. Ice Adhesion on Superhydrophobic Surfaces. *Appl. Surf. Sci.* **2009**, *255* (18), 8153−8157.
(35) Meuler, A. J.; Smith, J. D.; Varanasi, K. K.; Mabry, J. M.; McKinley, G. H.; Cohen, R. E. Relationships Between Water Wettability and Ice Adhesion. *ACS Appl. Mater. Interfaces* **2010**, *2* (11), 3100−10.
(36) Mishchenko, L.; Hatton, B.; Bahadur, V.; Taylor, J. A.; Krupenkin, T.; Aizenberg, J. Design of Ice-free Nanostructured Surfaces Based on Repulsion of Impacting Water Droplets. *ACS Nano* **2010**, *4* (12), 7699−7707.
(37) Varanasi, K. K.; Deng, T.; Smith, J. D.; Hsu, M.; Bhate, N. Frost Formation and Ice Adhesion on Superhydrophobic Surfaces. *Appl. Phys. Lett.* **2010**, *97* (23), 234102.
(38) He, M.; Wang, J.; Li, H.; Jin, X.; Wang, J.; Liu, B.; Song, Y. Super-hydrophobic film retards frost formation. *Soft Matter* **2010**, *6* (11), 2396−2399.
(39) Nosonovsky, M.; Bhushan, B. Superhydrophobic Surfaces and Emerging Applications: Non-adhesion, Energy, Green Engineering. *Curr. Opin. Colloid Interface Sci.* **2009**, *14* (4), 270−280.
(40) Kota, A. K.; Kwon, G.; Choi, W.; Mabry, J. M.; Tuteja, A. Hygro-responsive Membranes for Effective Oil-water Separation. *Nat. Commun.* **2012**, *3*, 1025.
(41) Yang, J.; Zhang, Z.; Xu, X.; Zhu, X.; Men, X.; Zhou, X. Superhydrophilic−superoleophobic Coatings. *J. Mater. Chem.* **2012**, *22* (7), 2834.
(42) Teare, P. W. The Crystal Structure of Orthorhombic Hexatriacontane $C_{36}H_{74}$. *Acta Crystallogr.* **1959**, *12* (4), 294−300.
(43) Koch, K.; Barthlott, W.; Koch, S.; Hommes, A.; Wandelt, K.; Mamdouh, W.; De-Feyter, S.; Broekmann, P. Structural Analysis of Wheat Wax (Triticum aestivum, c.v. "Naturastar" L.): from the Molecular Level to Three Dimensional Crystals. *Planta* **2006**, *223* (2), 258−70.
(44) Bhushan, B.; Koch, K.; Jung, Y. C. Biomimetic Hierarchical Structure for Self-cleaning. *Appl. Phys. Lett.* **2008**, *93* (9), 093101.
(45) Pechook, S.; Pokroy, B. Self-Assembling, Bioinspired Wax Crystalline Surfaces with Time-Dependent Wettability. *Adv. Funct. Mater.* **2012**, *22* (4), 745−750.
(46) Pechook, S.; Pokroy, B. Bioinspired Hierarchical Superhydrophobic Structures Formed by n-paraffin Waxes of Varying Chain Lengths. *Soft Matter* **2013**, *9* (24), 5710.
(47) Li, J.; Guo, Z.; Liu, J.-H.; Huang, X.-J. Copper Nanowires Array: Controllable Construction and Tunable Wettability. *J. Phys. Chem. C* **2011**, *115* (34), 16934−16940.
(48) Feng, J.; Qin, Z.; Yao, S. Factors Affecting the Spontaneous Motion of Condensate Drops on Superhydrophobic Copper Surfaces. *Langmuir* **2012**, *28* (14), 6067−75.
(49) Torresin, D.; Tiwari, M. K.; Del Col, D.; Poulikakos, D. Flow Condensation on Copper-based Nanotextured Superhydrophobic Surfaces. *Langmuir* **2013**, *29* (2), 840−8.
(50) Guo, Z.; Chen, X.; Li, J.; Liu, J. H.; Huang, X. J. ZnO/CuO Hetero-hierarchical Nanotrees Array: Hydrothermal Preparation and Self-cleaning Properties. *Langmuir* **2011**, *27* (10), 6193−200.
(51) Wen, X.; Zhang, W.; Yang, S. Synthesis of Cu(OH)2 and CuO Nanoribbon Arrays on a Copper Surface. *Langmuir* **2003**, *19* (14), 5898−5903.
(52) Wen, X. G.; Xie, Y. T.; Choi, C. L.; Wan, K. C.; Li, X. Y.; Yang, S. H. Copper-based Nanowire Materials: Templated Syntheses, Characterizations, and Applications. *Langmuir* **2005**, *21* (10), 4729−4737.
(53) Nosonovsky, M.; Bhushan, B. Roughness Optimization for Biomimetic Superhydrophobic Surfaces. *Microsyst. Technol.* **2005**, *11* (7), 535−549.
(54) Pan, S.; Kota, A. K.; Mabry, J. M.; Tuteja, A. Superomniphobic Surfaces for Effective Chemical Shielding. *J. Am. Chem. Soc.* **2012**, *135* (2), 578−81.
(55) Kota, A. K.; Choi, W.; Tuteja, A. Superomniphobic Surfaces: Design and Durability. *MRS Bull.* **2013**, *38* (05), 383−390.
(56) Nosonovsky, M.; Bhushan, B. Hierarchical Roughness Optimization for Biomimetic Superhydrophobic Surfaces. *Ultramicroscopy* **2007**, *107* (10−11), 969−79.

(57) Michael, N.; Bhushan, B. Hierarchical Roughness Makes Superhydrophobic States Stable. *Microelectron. Eng.* **2007**, *84* (3), 382−386.
(58) Bhushan, B.; Jung, Y. C.; Koch, K. Micro-, Nano- and Hierarchical Structures for Superhydrophobicity, Self-cleaning and Low Adhesion. *Philos. Trans. R. Soc., A* **2009**, *367* (1894), 1631−72.